Capillary Electrophoresis Measurements of the Free Solution Mobility for Several Model Polyelectrolyte Systems

D. A. Hoagland,* E. Arvanitidou, and C. Welch

Department of Polymer Science & Engineering, University of Massachusetts, Amherst, Amherst, Massachusetts 01003

Received March 12, 1999; Revised Manuscript Received July 19, 1999

ABSTRACT: The free solution electrophoretic mobilities of poly(styrenesulfonate), ss-DNA, and duplex DNA are measured by capillary electrophoresis across a range of ionic strengths and, for poly(styrenesulfonate) and ss-DNA, across a range of chain lengths. The data are then compared with mobilities reported in the literature and predicted by theory. For ionic strengths below 0.1 M, the capillary method is more accurate and rapid than previous techniques; it also provides a distribution of mobility values for polyelectrolyte mixtures. A maximum of the free solution mobility with respect to chain length is discovered in the oligomer range for both poly(styrenesulfonate) and ss-DNA; lowering ionic strength accentuates this unexplained phenomenon. In the large chain limit, where the mobility is independent of chain length, the ionic strength dependences of mobility for all three polymers are remarkably similar. These dependences can only be explained by models that incorporate nonlinear electrostatic effects into the description of the counterion cloud. The Manning model (with relaxation correction) best approximates the dependence of mobility on ionic strength.

Introduction

Techniques employing differences in electrophoretic mobility to separate and analyze polyelectrolyte mixtures have been available for over 60 years. Yet even where polyelectrolyte electrophoresis would appear simplest—in a free solution containing only small electrolyte ions—mobilities predicted by standard molecular-level theories may depart by 100% or more from those measured by experiment. Before electrophoretic techniques can be routinely considered for quantitative molecular *characterization*, above and beyond qualitative molecular *separation*, this large gap must be closed. We report here on the use of capillary electrophoresis to measure accurately the free solution mobility μ_0 of highly charged, water-soluble polyelectrolytes as a function of ionic strength I and degree of polymerization N. An earlier publication[1] described similar investigations of the role of chain charge density.

In the long term, we plan to generate a comprehensive μ_0 data set, one that can be confidently employed to assess and improve theories for polyelectrolyte electrophoresis. By studying the behaviors of multiple polyelectrolyte systems, we intend to isolate universal trends from those particular to a given polymer or solvent. Unexpected μ_0 behavior has often been attributed to specific interactions between polymer and small ions; if so, chemically dissimilar systems will exhibit different trends. In contrast, trends common to multiple polymer systems are more likely universal and thus predictable by conventional polymer solution models.

There are many reasons to conduct a systematic experimental study of polyelectrolyte electrophoresis in free solution. Recent theoretical advances in our understanding of gel electrophoresis and related techniques, for example, have assumed that μ_0 is independent of N. The rigor of this assumption remains unclear. In 1991, Cleland published a theoretical model[2] and data[3] suggesting that μ_0 increases with degree of polymerization N for values of N substantially beyond the normal oligomer range. Motivated in part by Cleland's report, and relying on an effective Gaussian approximation for intersegmental separations, Muthukumar developed an analytical theory for the field-induced transport of flexible polyelectrolyte chains.[4] In accord with Cleland's analysis, Muthukumar's theory predicted that μ_0 can exhibit a significant N dependence. Both conclusions challenge more prevalent experimental literature, i.e., that μ_0 does not depend on N beyond the oligomer regime. In an effort to resolve the discrepancy, Muthukumar formulated another electrophoresis theory, incorporating the intersegmental correlations of a charged polyelectrolyte through the chain structure factor.[5] (An equivalent theory was independently developed by Barrat and Joanny.[6]) This new theory predicts that μ_0 is indeed independent of N for large N. Most published data for uniformly charged polymers show that μ_0 increases to chain length independence for N greater than about 10−40.[7−12] Recently, however, Stellwagen et al. reported that μ_0 for duplex DNA rises with molecular weight M for chains containing up to 400 base pairs;[13] in an earlier report, Cohen et al. showed that differences in μ_0 allow duplex DNA restriction fragments of up to 23 000 base pairs to be separated electrophoretically in a complex, free solution environment.[14] We believe disagreement about the N dependence of μ_0 may be resolved by systematic experiments with lower N polyelectrolytes.

Poor understanding of the ionic strength I dependence of μ_0 raises related concerns. Even in the absence of specific, small ion−polymer interactions, the threshold for the N independence of μ_0 will be influenced by I, a factor unaddressed in previous experimental investigations of oligomer mobility. Theories for the mobility μ of polyelectrolytes in gels and similar media also neglect the impact of I. How will $\mu_0(I)$ track with $\mu(I)$? This sort of question must be addressed every time an electrophoretic procedure employing a new confinement matrix, polymer type, or buffer is developed. Most often, the question is solved empirically.[15]

10.1021/ma9903761 CCC: $18.00
Published on Web 08/25/1999

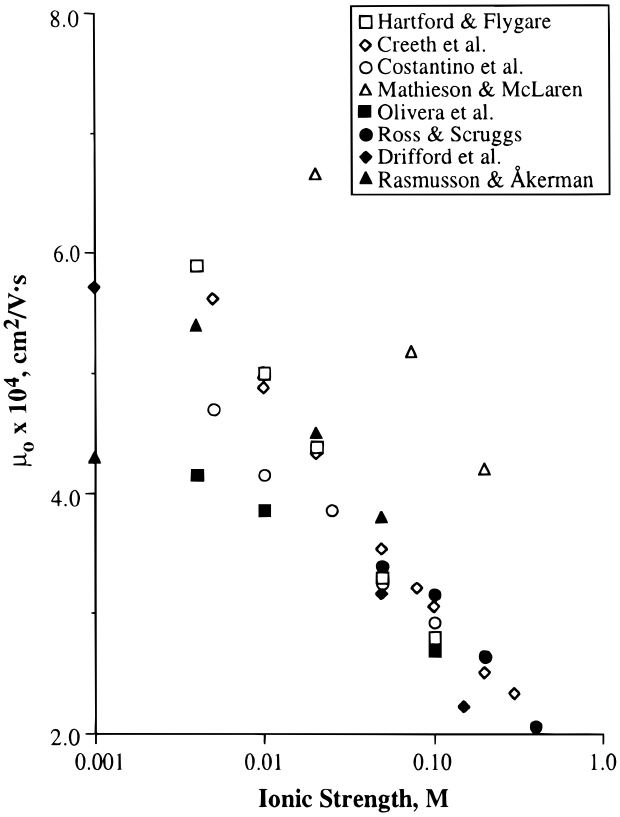

Figure 1. Electrophoretic mobility $\mu_0(I)$ for high molecular weight duplex DNA in aqueous NaCl. Data come from eight literature sources.[19,20,23−25,27,28,34]

Colloid scientists routinely employ free solution electrophoresis to characterize particle surface charge or potential, a practice that requires μ_0 to be transformed into microstructural information through a microscopic or molecular model. Such transformations are not yet possible for polyelectrolytes, because existing models are either insufficiently tested and/or unable to mimic the behavior of real systems. Definitive and comprehensive data for evaluating and developing new models have not appeared. Capillary electrophoresis may remedy this situation, with measurements of μ_0 at ±1−3% accuracy obtainable in 10−20 min. The method might conceivably make the electrophoretic characterization of polyelectrolyte charge as routine as the electrophoretic characterization of particle charge. However, practitioners of the method have focused on separation efficiency and/or development of new fractionation strategies, tasks that do not require rigorous control of experimental conditions or absolute knowledge of μ_0. For polyelectrolytes, capillary electrophoresis measurements of μ_0 have not, to our knowledge, been side-by-side compared with μ_0 values obtained by a more established experimental method.

The first relevant theory[16] and systematic experimental investigation[17] of polyelectrolyte electrophoresis appeared in the 1930s. Subsequent investigations of free solution electrophoresis have focused mostly on biopolymers,[3,7,8,13,18−34] but a significant number of synthetic polymers have also been examined.[1,28,35−47] Figure 1, compiling data from eight independent sources,[19,20,23−25,27,28,34] shows μ_0 as a function of I for high molecular weight duplex DNA in aqueous NaCl; this system has been studied most often. The large disparities in the data sets of Figure 1 plainly reveal why theoretical models for μ_0 have been so difficult to evaluate. Even more confusing, a maximum of μ_0 with I has been reported in a few cases.[33,34,37,40,42,43] Many literature data have been obtained in complex buffer or electrolyte systems which contain components that bind to the migrating polyelectrolyte.[13,36]

Theory

A. Overview of Physical Principles. The physical principles underlying polyelectrolyte electrophoresis are similar to those of classical colloid electrophoresis. In either case, one can separately consider the various forces acting on the migrating solute and, via force balance, generate an equation of motion.[48−50] Understanding this balance is crucial to a successful interpretation of the N and I dependences of μ_0.

The direct electric force $F_e = QE$, where Q is the charge and E is the applied field, is the most obvious force acting on a charged solute in an electrophoresis experiment. For a uniformly charged polyelectrolyte, this force is distributed evenly along the chain contour, exerting a force per unit length F_e/L, where L is the chain length. Nearly as obvious is the hydrodynamic drag force F_h which opposes field-induced migration in proportion to the solute's drift velocity. To model F_h, we imagine that the fluid surrounding the solute contains only neutral solvent, temporarily neglecting the presence of neighboring chains and small ions. In this hypothetical environment, F_h can be calculated as for a neutral solute. If the polyelectrolyte is spherical, F_h is given by Stokes' law, and if the chain is long and cylindrical, F_h is approximated by $3\pi\eta vL/\ln(L/2a)$, where η is the solvent viscosity, v is the steady-state cylinder velocity, and a is the cylinder radius. Unlike F_e, F_h is not distributed evenly along the chain contour.

In a real solution environment, solvated counterions possessing a total net charge $-Q$ form a diffuse cloud surrounding the polyelectrolyte, with the Debye length κ^{-1} characterizing the penetration of this cloud into the surrounding solution. For symmetric binary electrolytes of the type considered here,

$$\kappa^{-1} = \left(\frac{\epsilon kT}{2e^2z^2n_b}\right)^{1/2} \qquad (1)$$

where ϵ is the fluid permittivity, k is the Boltzmann constant, e is the electron charge, z is the ion valence, and n_b is the number of positive or negative ions per unit volume in the bulk. Each small ion experiences its own direct electric force of magnitude Eze, and these forces propagate throughout the surrounding fluid as spatially decaying velocity disturbances. Because the charge of the counterion cloud exactly compensates for the polyelectrolyte charge Q, the direct electric forces on the counterion cloud sum to $-F_e$; i.e., the net electrical force acting on a volume enclosing a solute and its counterion cloud is identically zero. However, the net retarding force F_c transmitted to the chain from counterions does not equal $-F_e$. Instead, the intervening viscous medium dampens the propagating disturbances as roughly the reciprocal of distance, making the magnitude of F_c less than F_e. Equation 1 shows that the characteristic distance between the chain backbone and its counterions depends on n_b, suggesting a strong influence of I on F_c. At high I, counterions cluster tightly to the chain and F_c is large, while at low I, counterions cluster less tightly and F_c is small. At the limit of zero

I, F_c entirely disappears. Information on the ion distribution relative to the central solute is needed to calculate F_c. This distribution can be derived from the nonlinear Poisson−Boltzmann equation or, more crudely, from the linearized Poisson−Boltzmann equation in the Debye−Hückel approximation.

The preceding arguments become invalid if the applied field, the local solvent flow, or the electromigration of counterions modifies the equilibrium structures of the chain or its ion cloud. Such modifications introduce nonlinearities into the analysis of solute motion. The electric and flow fields arising in a typical free solution electrophoresis experiment are orders of magnitude too small to perturb the equilibrium conformation of a flexible polyelectrolyte. Consequently, μ_0 can nearly always be considered insensitive to *E*, a feature permitting μ_0 values from different investigations to be directly compared. Perturbations to the structure of the ion cloud pose a more worrisome issue, since the cloud can be deformed at any field strength when the solute charge density is high. This deformation, reflecting both electromigration and convection of small ions, destroys the ion cloud's equilibrium fore−aft symmetry. One consequence is the displacement of the ion cloud's center of charge away from the solute's center of charge, a phenomenon creating a local dipole field oriented in opposition to the external electric field. The corresponding electrical counterforce F_r experienced by the solute due to this dipole field reduces solute mobility, an effect referred to as "relaxation". Distortions of the ion cloud must also be acknowledged as F_c is evaluated, with the needed corrections sensitive to the mobilities of the supporting electrolyte ions.

At steady state in a dilute polymer solution, the macroscopic force balance on a single polyelectrolyte chain can be written

$$F_e - F_h - F_c - F_r = 0 \tag{2}$$

Note that F_e and F_h can be computed separately, while F_c and F_r must generally be evaluated jointly since both depend on the ion cloud structure. Also note that F_e and F_r are exerted as electrical forces on the solute's charge sites, while F_h and F_c are felt across the solute's surface as distributed hydrodynamic forces. From the well-understood case of a charged sphere, one knows that all four terms in eq 2 can be important at large surface charge density.

If the ion cloud of a charged solute retains its equilibrium structure during free solution electrophoresis, F_r vanishes. This condition is met when the solute charge density is low enough to justify the Debye−Hückel approximation. Low charge density for a chain-like solute is established when the dimensionless charge density ξ

$$\xi = \frac{e^2}{4\pi\epsilon kTb} = \frac{l_b}{b} \tag{3}$$

is about unity or less. The ratio $e^2/4\pi\epsilon kT$ defines the Bjerrum length l_b, and *b* is the average axial distance between covalently bound charged groups ($b = Le/Q$). Values of ξ greater than unity define the class of highly charged polyelectrolytes. Using the Debye−Hückel approximation, the dimensionless surface potential ψ_s of a cylindrical chain segment can be written

$$\psi_s = 2\xi \frac{K_0(a\kappa)}{a\kappa K_1(a\kappa)} \tag{4}$$

where K_0 and K_1 are Bessel functions, and *a* is the effective segment radius. The surface potential has been made dimensionless with the ratio kT/e, and the charge has been smeared smoothly over the cylinder's "surface".

A complete Debye−Hückel description for electrophoresis of both spheres and cylinders was described by Henry in 1931;[16] his approach balances F_e, F_h, and F_c. Making μ_0 dimensionless with the ratio $2\epsilon kT/3\eta e$, Henry's solution for the dimensionless mobility μ_0' of an infinitely long cylinder can be expressed

$$\mu_0' = \psi_s \beta(a\kappa) \tag{5}$$

after equilibrium averaging over all cylinder orientations. The function $\beta(a\kappa)$ varies smoothly from 1.0 ($a\kappa = 0$) to 1.5 ($a\kappa = \infty$), and ψ_s can be taken from eq 4. For a typical polyelectrolyte possessing a backbone radius between 0.3 and 1.2 nm, the product $a\kappa$ falls in the range $10^{-4} < a\kappa < 1$, limiting β to values $1.0 < \beta < 1.10$. No distinction in these expressions has been made between a cylinder's hydrodynamic shear surface and its physical radius; if the two do not superimpose, the potential at the hydrodynamic shear surface, which defines the zeta potential, should be used in place of ψ_s.

Accepting the familiar Einstein relationship between *D* and μ_0,

$$\mu_0 = \frac{DQ}{kT} \tag{6}$$

the mobility of a charged cylinder might be expected to increase logarithmically with cylinder length *L* [i.e., $D \sim \ln(L)/L$, $Q \sim L$]. However, the parameter *L* does not appear in the formula for μ_0 derived by Henry. The reasons are simple: the Einstein relationship accounts only for F_h and F_e, while neglecting F_c and F_r. The derivation of Henry shows that the counterions responsible for F_c generate long-range hydrodynamic disturbances that exactly cancel the long-range hydrodynamic interactions generated by motion of cylinder segments; i.e., the direct electric force on a short cylinder segment generates a distant velocity disturbance exactly compensated by the distant velocity disturbance created by the direct electric forces on the nearby ion cloud. The usual segment−segment hydrodynamic interactions persist in the short range, however, where compensation is not complete. Indeed, the friction for a cylinder in an electrophoresis experiment reflects the local cylindrical surface geometry so long as $a\kappa \ll 1$.[51] Under this condition, and with $L\kappa \ll 1$, the Einstein relationship is strictly obeyed. Then, if lightly charged oligomers can be modeled as short cylinders, μ_0 can be expected to rise and then finally saturate to the *L*-independent Henry value for $L\kappa \gg 1$.

Attempting to exploit independent measurements of μ_0 and *D*, some investigators have forced the equality of eq 6 by interpreting *Q* as an "effective charge". The charge defined in this manner is almost always less than the real charge due to the retarding influences of F_c and likely F_r. The proper interpretation of mobility data requires a full accounting of forces, including F_e, F_h, F_c, and probably F_r. This assessment of eq 6 is not new[52] and not particular to polyelectrolytes.

B. Polyelectrolyte Specific Models. Insofar as polyelectrolyte electrophoresis is concerned, the classical Henry approach presents three major shortcomings: (1) the charge densities of most polyelectrolytes are too large for Debye−Hückel linearization, (2) many polyelectrolytes are inherently flexible, and (3) polymer chains are not infinitely long. A less significant criticism is the loss of local structural detail in a cylinder depiction, for example, the arbitrary smearing of charge over the cylinder surface when the charged sites are discrete. And, of course, one can level all the standard criticisms attached to any approach based on the Poisson−Boltzmann equation (finite ion size, application of the bulk dielectric constant in the region near the charged surface, replacement of the potential of mean force with the mean electrostatic potential, etc.). Last, and perhaps most subtly, the Henry model and most of its successors suppress or eliminate the Brownian motion of the central solute while retaining this motion for the small ions in the ion cloud; with polyelectrolytes, this inconsistent strategy can be questioned, especially for chain lengths in the oligomeric range.

The failure of Debye−Hückel linearization for large ξ can be redressed in two ways. In the first, Manning's concept of "counterion condensation" is applied; i.e., the backbone charge density is assumed to self-regulate via the strong association of counterions.[53] For $\xi > 1$, according to Manning's hypothesis, ion condensation in a 1:1 electrolyte will effectively reduce the dimensionless charge density to unity. A crude approximation for μ_0' can thus be obtained from eqs 4−5 by equating ξ to 1.0. (This assignment glosses over obvious uncertainties about the location of the shear plane relative to the population of condensed ions.) Manning incorporated counterion condensation in a more systematic fashion, replacing the cylinder model of Henry with a line of discrete, pointlike charges to obtain[54]

$$\mu_0' = \frac{6\pi\eta l_b}{\zeta} - 2\xi \ln\left[1 - \exp\left(\frac{-\kappa l_b}{\xi}\right)\right] \qquad (7)$$

where ζ is the friction coefficient associated with monomer electrophoresis, and counterion condensation restrictions apply to ξ (eq 7 is Cleland's elaboration of Manning's original formula[2]). Equation 7 lacks the relaxation effect, which Manning incorporated separately as a correction factor which grows in importance as the product κl_b is minimized.

Counterion condensation, as an ad hoc hypothesis, does not offer the rigor ascribed to a formal solution of the nonlinear Poisson−Boltzmann equation using a Gouy−Chapman description for the ion cloud. Unfortunately, a full Poisson−Boltzmann solution for a flexible, highly charged polyelectrolyte in an electric field does not exist. As an alternative, ion distributions near a long charged cylinder have been calculated from the nonlinear Poisson−Boltzmann equation and these distributions employed to calculate F_c and F_r for $\xi > 1.0$. Following a formalism developed by Wiersema et al.,[48] Schellman and Stigter[55−59] developed a numerical scheme to implement this approach. Unlike Manning, they found that the relaxation effect lowers μ_0' only at intermediate values of $a\kappa$, with the extent of the reduction dependent on ψ_s; with ψ_s small enough for Debye−Hückel linearization, the effect disappears. In fact, the trends predicted for a cylinder using the full Poisson−Boltzmann equation closely parallel the classical trends predicted for a sphere, if cylinder radius a is substituted for sphere radius R.[48]

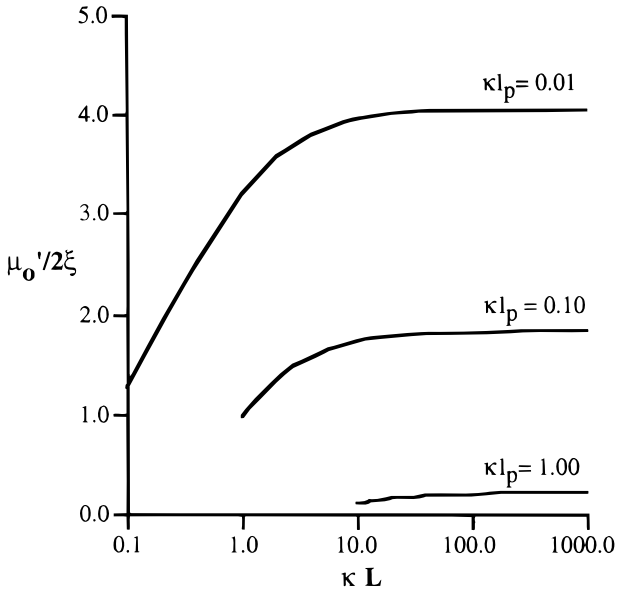

Figure 2. Dimensionless mobility $\mu_0'(\kappa L)$ given by the Muthukumar solution for rodlike chains.

On physical grounds, the greatest objection to either the Manning, Henry, or Stigter approaches for the case of flexible polyelectrolytes would appear to be the neglect of backbone flexibility. Flexibility at the level of a wormlike chain was added to Stigter's analysis by Cleland, with surprisingly little impact on μ_0' noted.[2] More recently, Muthukumar[5] used the Debye−Hückel approximation to solve for μ_0 of a linear chain characterized by structure factor $S(k)$, radius of gyration R_g, and segment size l_p. His general result, accounting for both backbone flexibility and finite chain length, can be expressed

$$\mu_0' = \frac{2\xi}{\pi}\int_0^\infty \frac{(kl_p)^2}{(kl_p)^2 + (\kappa l_p)^2} S(kR_g) l_p \, dk \qquad (8)$$

An exact expression for $S(k)$ is available for rodlike chains, allowing an explicit evaluation of the integral. This approach leads to the formula

$$\mu_0' = 2\xi\left\{E_1(\kappa l_p) - E_1(\kappa L) - \left(\frac{1}{\kappa L}\right)[1 - \exp(-\kappa L)]\right\} \qquad (9)$$

where E_1 is the exponential integral. For large κL, eq 9 agrees with Henry's formula in its small $a\kappa$ limit (albeit with cylinder radius a replaced by segment size l_p). The equation also provides the expected logarithmic L dependence for short enough chains, as shown in Figure 2. Völkel and Noolandi[10,60] and Allison and Mazur[61] derived molecular weight dependences for single-stranded DNA using more structurally realistic molecular models.

To model flexible chains, Muthukumar approximated $S(k)$ with an interpolation formula, rigorously valid only at small and large kR_g. Substituting into eq 9 and then evaluating the integral in the experimentally accessible limit for a coiled molecule, i.e., $\kappa R_g \gg 1$, he found

$$\mu_0' = \frac{\xi}{\pi}\left(\frac{3}{2\nu}\right)^{1/2\nu} (l_p\kappa)^{1-1/\nu} \Gamma\left(\frac{3 - 1/\nu}{2}\right) \Gamma\left(\frac{1/\nu - 1}{2}\right) \qquad (10)$$

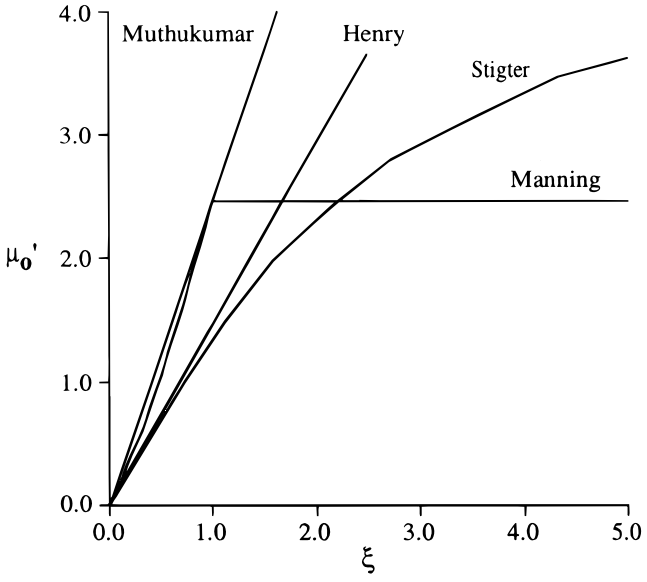

Figure 3. Dimensionless mobility $\mu_0'(\xi)$ for four models ($a\kappa = \kappa l_b = \kappa l_p = 1.0$; for Stigter $m_\pm = 0.184$; for Manning $\zeta = 3\pi\eta b$; for Muthukumar $\nu = 3/5$).

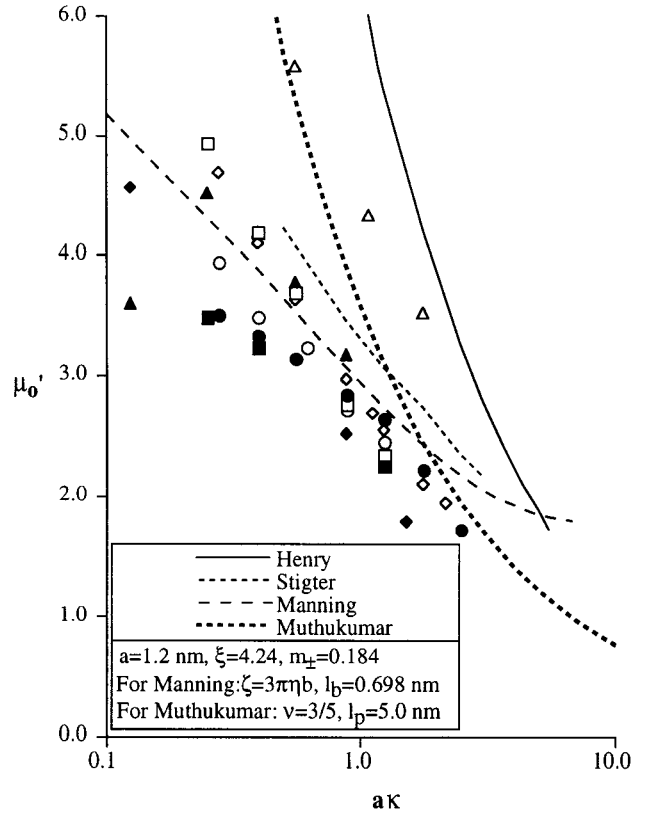

Figure 4. Dimensionless mobility $\mu_0'(a\kappa)$ for high molecular weight duplex DNA compared to four models. Symbols for data are as given in Figure 1.

where Γ is the gamma function and $\nu < 1$. Equation 10 predicts a molecular weight independent mobility that decreases with κ as a power law; more specifically, assuming $\nu \approx 3/5$, μ_0' decreases as $\kappa^{-2/3}$. In contrast, irrespective of model, when the Debye−Hückel approximation is made for a slender rodlike solute, the mobility decreases as $-2\xi \log(\kappa)$.

Figures 3 and 4 display the dependence of μ_0' on ξ and $a\kappa$, respectively, for the Henry, Stigter, Manning, and Muthukumar models. (Because the models incorporate different physical parameters, construction of the two figures requires that several geometric factors be assumed; these assumptions have a minor consequence for the current discussion. Also, the possible presence of a Stern layer is ignored.) After the appropriate reductions to dimensionless form, Figure 4 superimposes the same experimental data for duplex DNA presented in Figure 1. Determining which of the models best describes the data is clearly problematic. Not surprisingly, one concludes that the two models employing the Debye−Hückel approximation substantially overstate the $a\kappa$ dependence of μ_0'.

Additional theories for polyelectrolyte electrophoresis have been developed by Hermans and Fujita[62,63] (porous sphere model), Overbeek and Stigter[64] (porous sphere model), Takahashi et al.[39] (Poisson−Boltzmann rod model without relaxation effects), Abramson et al.[18] (Debye−Hückel rod model with incorrect orientational averaging), Mills[65] (Poisson−Boltzmann rod model with incorrect orientational averaging and no relaxation effects), Imai and Iwasa[66] (free-draining Poisson−Boltzmann coil model with unspecified chain friction constant), Schmitt et al.[67,68] (phenomenological Debye−Hückel theory invoking empirical binary friction coefficients), van der Drift et al.[69] (Poisson−Boltzmann rod model with semiempirical relaxation correction), Long et al.[70,71] (Zimm model with localized forces and no relaxation correction), and Allison et al.[61,72,73] (boundary element methodology to describe the hydrodynamics and Poisson−Boltzmann electrostatics of arbitrarily shaped and charged rigid polyions).

Experimental Section

A. Materials. The polyelectrolytes examined by free solution electrophoresis include poly(styrenesulfonate) [PSS] (Pressure Chemical Co.), intact λ phage duplex DNA (GIBCO BRL), phosphorylated poly(deoxythymidine) [poly(dT)] (Sigma), and single-stranded DNA produced by denaturation of calf thymus duplex DNA (Sigma). Degrees of polymerization for anionically polymerized PSS range from 8 to 5150, while oligomers (N = 2, 4, 6, 8, and 16) and polymer ($N > 650$) are available for poly(dT). The λ phage DNA is monodisperse ($M = 33 \times 10^6$ g/mol [48 502 base pairs]), and the ss-DNA is a polydisperse mixture with an average M in the millions. Experiments have also been performed with poly(acrylic acid) and its copolymers with poly(acrylamide), but the results have been presented elsewhere.[1] The model compound selected to mimic the behavior of PSS unimer ($N = 1$) is styrenesulfonate (Pressure Chemical).

Preliminary experiments found that the as-received λ phage duplex DNA was contaminated with protein and/or RNA, species that interfere with UV/vis detection of DNA. Duplex DNA samples were thus initially purified by phenol−chloroform extraction. The treated samples were stored at 4 °C until a few hours prior to use, when they were heated briefly to 65 °C to remove linear aggregates and/or cyclics. Irrespective of polymer type, samples obtained as solid powders were dissolved directly in the chosen run electrolyte, and those obtained as solutions extensively dialyzed against this electrolyte for 2−3 days. The background electrolyte used for all studies reported here was either NaCl or Na_2HPO_4. Polymer concentrations were between 0.05 and 0.3 mg/mL. At these dilute concentrations, added low molecular weight salts effectively dictate electrolyte conditions for $I \geq 0.001$ M, and I was calculated from the concentrations of these salts. For studies of $I < 0.001$ M, polymers were dissolved in deionized water with no added background electrolyte so that the ionic strength of the polymer sample solution would closely match that of the running buffer solution.

B. Equipment. Our capillary electrophoresis experiments are performed in a home-built apparatus that combines a CV[4]

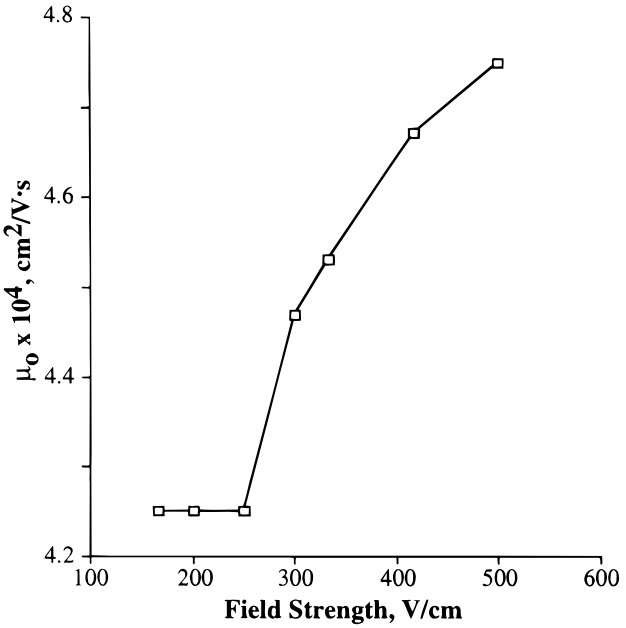

Figure 5. Apparent electric field dependence of the electrophoretic mobility of high molecular weight PSS in aqueous Na_2HPO_4 (I = 0.03 M); the rise at 250 V/cm can be attributed to Joule heating of the solution.

UV/vis detector from ISCO with a 0−30 kV power supply from Glassman High Voltage. Fused silica capillaries of 50 μm internal diameter are purchased from Polymicro Technologies and cut to the appropriate length, typically 60−100 cm. Capillaries in our apparatus are housed in an electrically interlocked Plexiglas housing attached to the side of the ISCO detector. The housing contains two fans, the more powerful recirculating the entire interior atmosphere through a water-cooled automobile heater core. The heater core acts as a water-to-air heat exchanger, using water pumped at 3 L/min from an external 20 L chilled bath. The air temperature in the interlocked compartment is continuously monitored, with fluctuations typically noted at the level of ±0.2 °C over the course of a day. The second fan blows the cooled interior air at high velocity directly at the active segment of the free-standing capillary.

Reproducible mobility measurements do not guarantee the absence of a temperature problem due to Joule heating. To validate each measurement, we routinely monitor two functions: the current−voltage relationship of the solvent-filled capillary and the apparent electric field dependence of μ_0. Since the second function can be determined only through a sequence of lengthy trials, the current−voltage relationship is always assessed first. Although solvent composition exerts a strong influence, we generally find via these tests that resistive heating can be neglected for electric fields less than 250 V/cm, as shown in Figure 5. At salt concentrations higher than 0.1 M, μ_0 becomes difficult or impossible to measure because run times are so long (>1−2 h) that reproducibility cannot be confirmed. Only data triply reproduced in series are reported. We are confident that all of the measurements reported in this article correspond to solution temperatures of 20.0 ± 0.2 °C.

C. Procedures. Measurement reproducibility for these nonadsorbing[74] polymers can be enhanced by exposing and oxidizing the capillary's bare glass surface, creating the maximum possible fraction of negative silanol groups. Using a microsyringe for injection, flushing of a new fused silica capillary begins with a 1 h exposure to 1.0 M NaOH followed by a 15 min exposure to 0.01 M NaOH. Next, several capillary volumes of run buffer or background electrolyte solution are injected by the same procedure. Final equilibration of the capillary with this fluid occurs in the presence of an applied field (≤250 V/cm). When reproducibility becomes poor, the conditioning sequence is repeated. Problems are typically manifested as a reduction in electroosmotic flow, indicating that a neutral contaminant has attached to the capillary wall. The frequency of reconditioning depends on the polymer system tested, and reconditioning occasionally may be required as often as every other run or as infrequently as once every few days. During overnight periods, the capillary is filled with 0.01 M NaOH. All filling and test solutions are filtered through 0.22 μm Millex-GV filters (Millipore) just prior to use.

Even with these time-consuming preliminaries, anomalous results are occasionally encountered. As an additional check on run conditions, the conductivity of each new electrolyte solution is determined in a gold dip cell attached to a conductivity meter (Cole-Parmer). The conductivity measured in this cell is compared to the theoretical value given by Kohlrausch's law of independent ion migration. Although strictly valid for dilute electrolytes, we find Kohlrausch's law quantitatively satisfied by our electrolyte systems for I as large as 0.05 M. Solutions with ionic strengths below 0.05 M that do not possess conductivities within ±5% of Kohlrausch's law are immediately discarded. After placing the accepted solutions in the capillary, a second conductivity value is determined using the current and voltage read from the power supply. If the new conductivity value deviates by more than ±20% from that measured in the dip cell at any point during measurement, a new solution or capillary is prepared.

Electrokinetic sample injection occurs at the anode (positive polarity), regardless of polyelectrolyte charge, because the negative capillary surface drives an electroosmotic velocity V_{osm} exceeding the sample's opposing electrophoretic velocity V_{el}. Injection time varies according to run condition, but 5−10 s is a nominal time to insert 10 nL of sample. At the polymer concentration required for absorbance detection (0.05−0.3 mg/mL), such a volume contains about 0.5−3 ng of polymer. The injected material migrates under the combined influence of electrophoresis and electroosmosis, with the net solute velocity V_{net} given by

$$V_{net} = V_{osm} - V_{el} \tag{11}$$

Since V_{el} values are the experimental objective, V_{osm} is separately measured using a co-injected neutral tracer (acetone). Figure 6A displays a typical electropherogram (concentration vs time) for λ DNA. The time variable of the figure can be converted to μ_0 by the definition of μ_0 as V_{el} divided by the applied field E; Figure 6B displays the resulting μ_0 distribution. We believe the breadth of the μ_0 peak results mainly from the finite sample injection volume, with a smaller contribution from polymer diffusion during passage through the capillary. For these polymers, peak position always defines an unambiguous μ_0 value to an accuracy of ±3%. Samples expected to display a single, well-defined value of μ_0 always produce a single, narrow electropherogram peak, a behavior suggesting that electromigration and other anomalous effects are unimportant. Polyelectrolyte and counterion contributions to the conductivity become important only at lower ionic strengths than examined here; these contributions can make μ_0 measurement by CE difficult. Absorbance is monitored at 235 nm for PSS and 260 nm for DNA.

To verify the entire measurement strategy, a limited set of duplicate μ_0 data for PSS have been generated by electrophoretic light scattering (ELS). The ELS method exploits the Doppler shift in solute scattered light to determine electrophoretic motion. With a Delsa 440 ELS instrument (Coulter Electronics), the shift is followed at four widely spaced scattering angles, an approach that enables four redundant measurements of solute velocity at the stationary plane of a rectangular electrophoresis cell. Unfortunately, since the Delsa 440 instrument was designed for particle electrophoresis, the incident intensity is low, making operation for highly diluted polymers difficult. With PSS, weak polymer scattering makes the measurement of μ_0 impossible for NaCl concentrations below about 0.001−0.005 M. (The exact I threshold is M-dependent.) A limiting μ_0 value is therefore inferred by extrapolating ELS measurements made at polymer concentrations in the range 1−10 mg/mL. Because of these constraints,

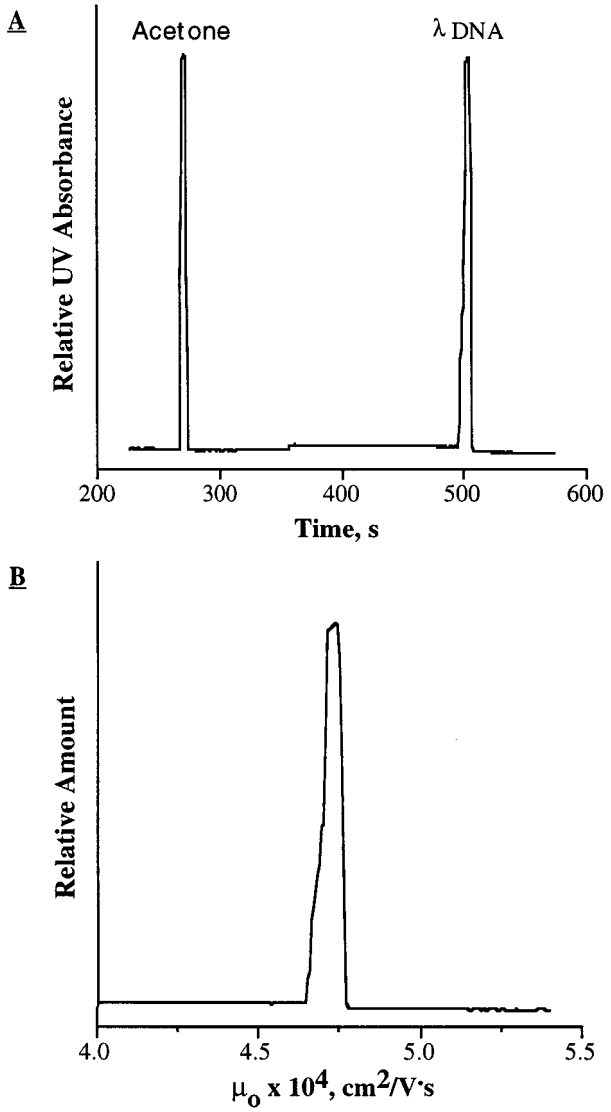

Figure 6. (A) Typical electropherogram for λ DNA in aqueous NaCl, with acetone as the co-injected neutral tracer. (B) Mobility distribution for the λ DNA of (A).

overlapping measurements for PSS by the two techniques are only possible over a range roughly 0.003 M < I < 0.3 M.

Results and Discussion

A. Molecular Weight Trends. We have systematically examined μ_0 as a function of M for PSS and poly(dT), polymers widely documented for their M-dependent μ behaviors in poly(acrylamide) and/or agarose gels. Both polymers are intrinsically flexible, available in nearly monodisperse fractions, and highly charged. The intrinsic persistence length and ξ for PSS are roughly 1.2−1.4 nm[75,76] and 2.50−2.78,[76] respectively, while for poly(dT) the corresponding values will be similar to those reported for ss-DNA, roughly 1.0 nm and 1.65, respectively.[77,78] Incorporating electrostatic contributions, the persistence length at lower I will be larger.

Figure 7 shows the N dependence of μ_0 for PSS; the data come from both capillary electrophoresis and ELS. Irrespective of technique, the same N trend is observed over the entire I range examined (0.0001 M < I < 3.0 M), with μ_0 independent of N within experimental error for N > 100. Trends at lower N are complex. As seen in

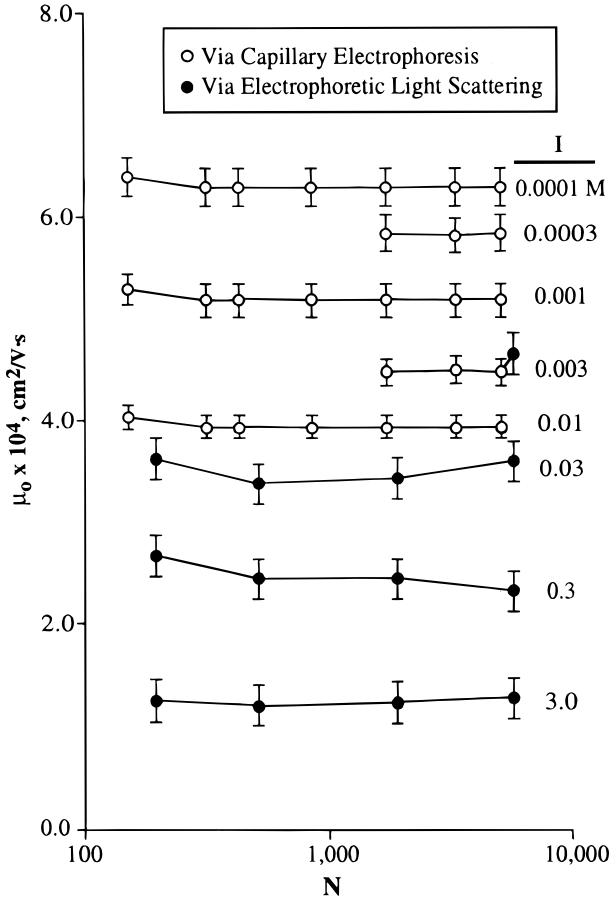

Figure 7. Electrophoretic mobility $\mu_0(N)$ for PSS in aqueous NaCl with N > 100. Reproducibility of sequential runs is reflected in ±1.0 standard deviation error bars.

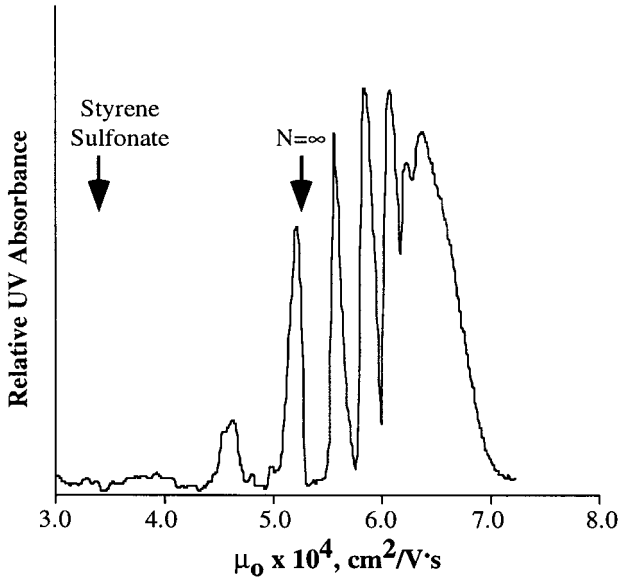

Figure 8. Mobility distribution for PSS with nominal N = 8 and I = 0.001 M in aqueous NaCl. Arrows indicate mobilities measured for styrenesulfonate (N = 1) and high molecular weight PSS (N = ∞) when co-injected with the N = 8 PSS; these mobility values were verified in separate runs of individual styrenesulfonate and high molecular weight PSS, using identical run conditions.

Figure 8, one of the low-N fractions with nominal degree of polymerization 8 produces multiple electropherogram peaks. Such peaks can most readily be interpreted as

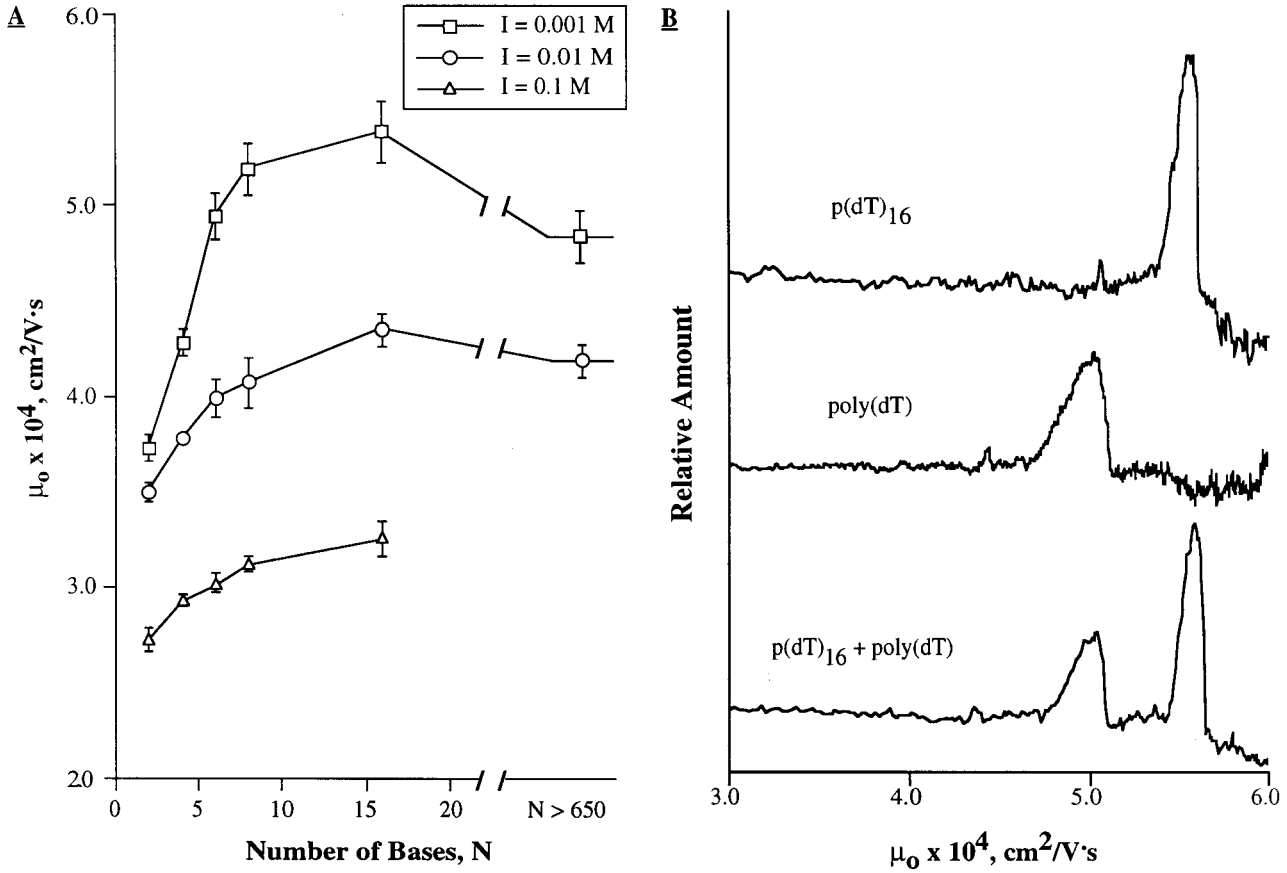

Figure 9. (A) Mobility $\mu_0(N)$ for poly(dT) in aqueous Na_2HPO_4. Reproducibility of sequential runs is reflected in ±1.0 standard deviation error bars. (B) Mobility distributions at $I = 0.001$ M for monodisperse oligomeric poly(dT) with $N = 16$, high molecular weight poly(dT) ($N > 650$), and a mixture of the two.

an electrophoretic separation by N. With the electropherogram shape insensitive to sample concentration, the multiple peaks cannot be attributed to electromigration and other anomalous dispersion phenomena. Surprisingly, some of the peaks correspond to μ_0 greater than that of either styrenesulfonate or high-N PSS; this electropherogram, together with those for other oligomeric PSS samples, suggests that μ_0 passes through a maximum somewhere in the range $5 < N < 25$. Unfortunately, as we are unable to assign N values unambiguously to the different electropherogram peaks, the maximum and its location remain speculative. Standard elemental analysis and MALDI mass spectroscopy confirm the chemical identity and the nominal chain length of the PSS samples displaying this type of low-N behavior. Multiple peaks or anomalous breadth for a single polymer peak are not observed for PSS samples with M above 10 000 g/mol.

More conclusive low-N information is obtained for oligomers and polymer of poly(dT). Figure 9A plots $\mu_0(N)$ for poly(dT), using I as a parameter. For poly(dT), N-dependent μ_0 is confined to short chains, with the observed behavior highly dependent on I. As expected from the introductory discussion, μ_0 rises with N in the low-N range, reflecting an increasing compensation of hydrodynamic effects as the chain size grows relative to κ^{-1}. The difference between μ_0 of polymer and dimer reduces with I; the difference at the lowest I examined ($I = 0.001$ M) is 24%, a value roughly consistent with the difference between polymer and monomer for PSS mobility. At low I, the maximum in μ_0 for poly(dT) is unambiguous. For $I = 0.001$ M, the mobility at $N = 16$ is roughly 20% greater than for the high molecular weight polymer, which, as Figure 9B establishes, is a sufficient mobility difference to allow the two samples at this condition to be electrophoretically baseline separated when mixed. The magnitude of the mobility maximum appears to diminish at larger I, although data for these conditions are more limited. A lack of monodisperse samples in the range $16 < N < 600$ prevents the location of the mobility maximum to be established more accurately.

Perturbations from end groups are frequently a concern in oligomer studies. By MALDI mass spectroscopy, the PSS chains are determined to possess a butyl group on one chain end and a proton on the other. Phosphorylation of the poly(dT) oligomers adds one extra phosphate group to a single chain end (in addition to the phosphate for each repeat unit). We have been unable to formulate a simple chain model that would predict a mobility maximum when an extra charge or frictional unit is placed at the chain end(s). In addition, since PSS and poly(dT) differ so greatly in end group structure and yet show the same oligomer behavior, we do not believe the functionality on the chain end is responsible for the mobility maximum we observe.

The only data in the literature that might be compared to ours are those of Grossman,[7] who studied poly(dT) by capillary electrophoresis as well. Although his data are roughly comparable to those presented here, with mobility rising with N in the range $2 < N < 10$, no maximum in μ_0 is noted. We believe that a combination of Joule heating and high ionic strength in his study suppressed the maximum we see; also, the composition

of Grossman's buffer was totally different than the one employed here. For duplex-DNA, Stellwagen[13] also did not report a maximum. However, the large stiffness of duplex-DNA probably invalidates any comparison to results for ss-DNA.

Irrespective of possible ambiguities in data interpretation, or in matching theory to experiment, the current experimental results conclusively establish that μ_0 for flexible polymers is totally independent of N beyond the oligomer range. The mobility for oligomers generally rises with N, saturating when this parameter reaches approximately 20−50. The presence of the maximum in the mobility at intermediate N will clearly be an enormous hindrance to the use of free solution electrophoresis for separating polyelectrolyte oligomers. Unfortunately, the presence of the maximum may not always be immediately obvious. None of the theoretical models discussed earlier predict a maximum, so we do not plot theoretical fits to the data here.

B. Ionic Strength Trends. Many investigators have attempted to examine $\mu_0(I)$ for high-N polymers, but the basic trends in this function remain uncertain, as most often the range of I has been unduly restricted or the electrolyte conditions have been improperly monitored. The latter issue becomes especially important at low I ($I < 0.0001$ M), where inadvertent impurities can raise I above the level calculated from the concentration of deliberately added salt. These problems raise serious concerns about literature data sets, as illustrated in the confusing trends noted in Figure 1. Any characteristic feature in the function $\mu_0(I)$, such as a change in slope, reflects a characteristic molecular dimension (i.e., one comparable to κ^{-1} at that I). At ordinary ranges of I ($0.0001\ \text{M} < I < 1.0$ M), the structures of a chain and its surrounding atmosphere are probed by electrophoresis at length scales comparable to or slightly larger than the backbone radius. At even lower I, analogous experiments will probe larger length scales, perhaps those approaching the radius of gyration. Since overall chain dimensions decrease with increasing I, rather complicated $\mu_0(I)$ trends can be anticipated. Experiments in this study are limited to $I > 0.0001$ M, to avoid the issues of ionic impurities and salt-free chain dynamics. Polymer solutions are prepared at concentrations well below coil overlap, avoiding chain entanglements and permitting I to be calculated without regard for the fraction of mobile counterions.

Figures 10−12 display $\mu_0(I)$ for long chains of PSS, duplex DNA, and ss-DNA. For PSS, the mobilities measured by capillary electrophoresis and electrophoretic light scattering show excellent agreement, verifying our ability to measure μ_0 quantitatively via capillary electrophoresis. For DNA, our experimental data fall roughly into the middle of the data shown in Figure 4; to avoid confusion, these literature data are not superimposed on the new plot. The lowest ionic strength probed in our experiments (0.0001 M) is an order of magnitude lower than any other study with DNA.

To compare experimentally measured mobilities to those predicted by theory, μ_0 and I must be converted to their dimensionless counterparts, μ_0' and $a\kappa$ (as in Figure 4). Assigning a value for the backbone radius a is not straightforward; therefore, we do so only for duplex DNA, which has been extensively characterized. Figure 11 compares our experimental results for duplex DNA to the predictions of Manning[54] and Stigter,[55−59]

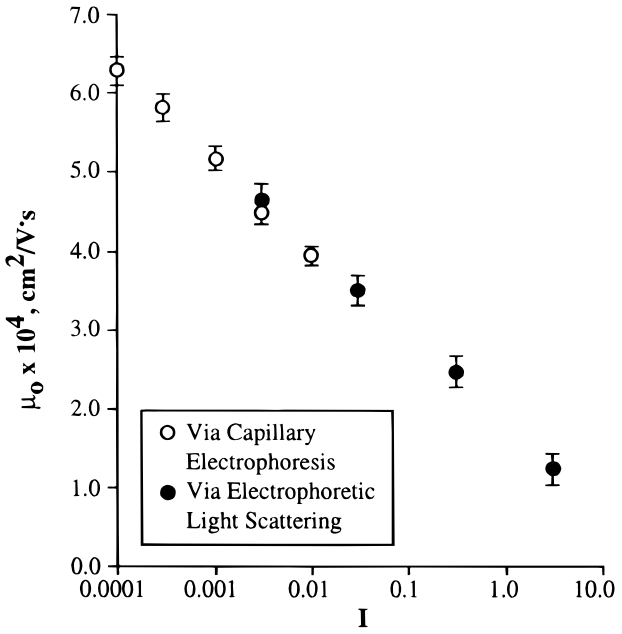

Figure 10. Mobility $\mu_0(I)$ for high molecular weight PSS in aqueous NaCl. Reproducibility of sequential runs is reflected in ±1.0 standard deviation error bars.

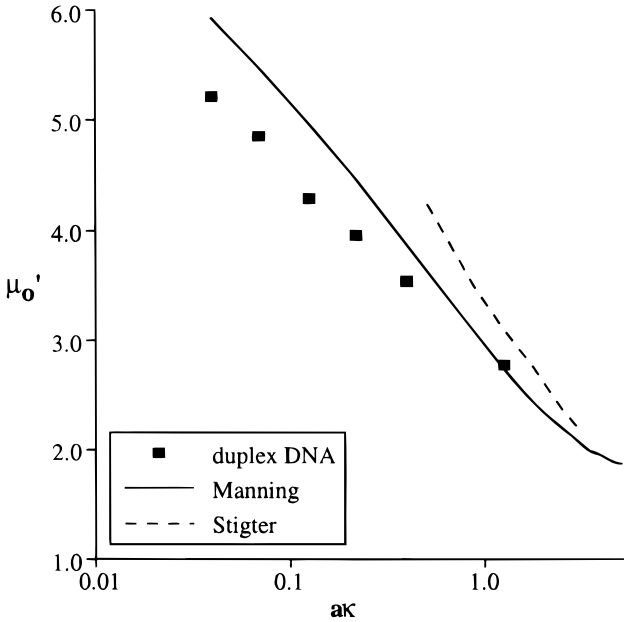

Figure 11. Dimensionless mobility $\mu_0'(a\kappa)$ for high molecular weight duplex DNA in aqueous NaCl compared to the Manning and Stigter models ($a = 1.2$ nm, $\xi = 4.24$; for Manning $\zeta = 3\pi\eta b$, $l_b = 0.698$ nm; for Stigter $m_\pm = 0.184$).

which both show reasonable agreement to our data. (The Stigter model is limited to higher values of $a\kappa$ due to the limited range of published tabulations.) In both cases, relaxation effect corrections have been applied, which improves the agreement between theory and experiment. However, while the relaxation effect amounts to only a 10−20% correction of overall mobility for the Stigter model, the same correction is much larger for the Manning model, especially at lower I; for the Manning model, the relaxation effect in the extreme case amounts to a 50% correction to eq 7. In absence of an accounting for the relaxation effect, the Manning model agrees no better with the data than does the Stigter model. The relaxation effect incorporated into

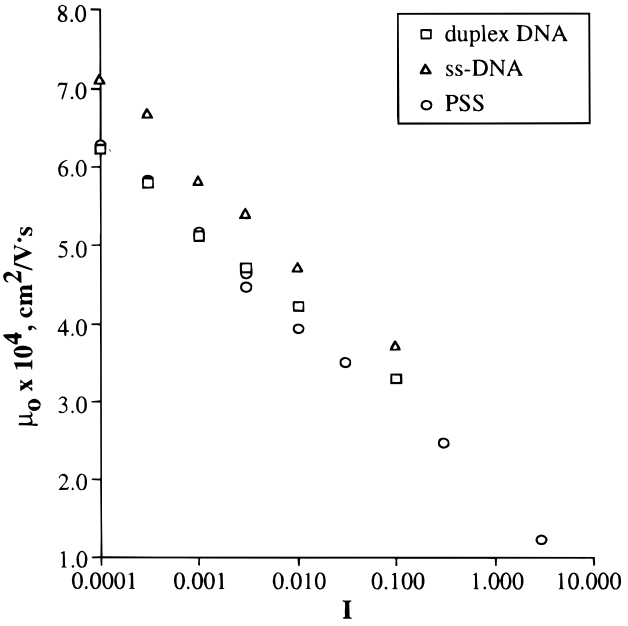

Figure 12. Superposition of mobility $\mu_0(I)$ for the three polyelectrolytes of this study, in aqueous NaCl.

the Manning model appears to be physically different than the one evaluated in the Stigter model.

Figure 11 appears remarkably similar to Figure 10, although the corresponding polymers are structurally very different. Figure 12 reveals an apparent and unexpected universality as we compare $\mu_0(I)$ for the three polyelectrolytes of our study—PSS, duplex DNA, and ss-DNA: μ_0 varies more significantly with I than with chemical structure, even when these structures are substantially different. The behavior of PSS, in fact, is more comparable to duplex DNA than ss-DNA, which PSS more closely resembles in physical properties. Furthermore, except at extremely low I, literature results for the mobility of poly(vinyl sulfate)[37] and poly(acrylic acid)[40] can be neatly overlapped onto the data of Figure 12 after suitable correction for temperature differences between experiments. To be totally objective about this overlap, we must note that other literature data sets[26,28,42] do not superimpose so well in this I regime. However, these poorly superimposing data mostly come from studies characterized by large experimental error. (Figures 1 and 4 graphically display why literature comparisons are so difficult.) In contrast to some earlier studies,[33,34,37,40,42,43] we see no indication of a peak in $\mu_0(I)$ at low I; we believe a maximum may arise from poor control of electrolyte composition at low I.

Summary

The N and I dependences of μ_0 have been measured by capillary electrophoresis for well-characterized polyelectrolytes. With careful attention to temperature control, the method rapidly returns accurate and absolute measurements of μ_0. For high molecular weight polymers, μ_0 is N-independent; for flexible oligomers, behavior is more complex, and $\mu_0(N)$ exhibits a maximum with respect to N when I is low. The physical basis for this maximum is currently unknown, although backbone flexibility may play an important role.[79] The dependence of μ_0 on I can only be explained by theories that account for electrostatic nonlinearities. Somewhat surprisingly, the I dependences of μ_0 are quantitatively similar for polymers of different chemical structure. This overlapping implies that the discrepancies between theory and experiment in the function $\mu_0(I)$ cannot be explained by specific polymer−ion association.

Acknowledgment. We appreciate the financial support given this study by the UMass MRSEC and the discussions we have had on this topic with Prof. M. Muthukumar. David Smisek gathered some of the electrophoretic light scattering data.

References and Notes

(1) Hoagland, D. A.; Smisek, D. L.; Chen, D. Y. *Electrophoresis* **1996**, *17*, 1151−1160.
(2) Cleland, R. L. *Macromolecules* **1991**, *24*, 4391−4402.
(3) Cleland, R. L. *Macromolecules* **1991**, *24*, 4386-4390.
(4) Muthukumar, M. *Macromol. Theory Simul.* **1994**, *3*, 61−71.
(5) Muthukumar, M. *Electrophoresis* **1996**, *17*, 1167−1172.
(6) Barrat, J.-L.; Joanny, J.-F. In *Advances in Chemical Physics*; Prigogine, I., Rice, S. A., Eds.; John Wiley: New York, 1996; Vol. 94, pp 1−62.
(7) Grossman, P. D. In *Capillary Electrophoresis: Theory and Practice*; Grossman, P. D., Colburn, J. C., Eds.; Academic Press: San Diego, CA, 1992.
(8) Dolnik, V.; Liu, J.; Banks, J. F., Jr.; Novotny, M. V.; Boček, P. *J. Chromatogr.* **1989**, *480*, 321−330.
(9) Carney, S. L.; Osborne, D. J. *Anal. Biochem.* **1991**, *195*, 132−140.
(10) Völkel, A. R.; Noolandi, J. *Macromolecules* **1995**, *28*, 8182−8189.
(11) Braud, C.; Vert, M. *Polym. Bull.* **1992**, *29*, 177−183.
(12) Cohen, A. S.; Terabe, S.; Smith, J. A.; Karger, B. L. *Anal. Chem.* **1987**, *59*, 1021−1027.
(13) Stellwagen, N. C.; Gelfi, C.; Righetti, P. G. *Electrophoresis* **1997**, *42*, 687−703.
(14) Cohen, A. S.; Najarian, D.; Smith, J. A.; Karger, B. L. *J. Chromatogr.* **1988**, *458*, 323−333.
(15) Smisek, D. L.; Hoagland, D. A. *Macromolecules* **1989**, *22*, 2270−2277.
(16) Henry, D. C. *Proc. R. Soc. London, Ser. A* **1931**, *133*, 106−140.
(17) Tiselius, A. *Trans. Faraday Soc.* **1937**, *33*, 524−531.
(18) Abramson, H. A.; Moyer, L. S.; Gorin, M. H. *Electrophoresis of Proteins*; Reinhold Pub. Corp.: New York, 1942.
(19) Creeth, J. M.; Jordan, J. O.; Gulland, J. M. *J. Chem. Soc. (London)* **1949**, 1406−1409.
(20) Mathieson, A. R.; McLaren, J. V. *J. Chem. Soc. (London)* **1956**, 303−307.
(21) Ross, P. D. *Biopolymers* **1964**, *2*, 9−14.
(22) Ross, P. D.; Scruggs, R. L. *Biopolymers* **1964**, *2*, 79−89.
(23) Ross, P. D.; Scruggs, R. L. *Biopolymers* **1964**, *2*, 231−236.
(24) Olivera, B. M.; Baine, P.; Davidson, N. *Biopolymers* **1964**, *2*, 245−257.
(25) Costantino, L.; Liquori, A. M.; Vitagliano, V. *Biopolymers* **1964**, *2*, 1−8.
(26) Tuffile, F. M.; Ander, P. *Macromolecules* **1975**, *8*, 789−792.
(27) Hartford, S. L.; Flygare, W. H. *Macromolecules* **1975**, *8*, 80−83.
(28) Drifford, M.; Menez, R.; Tivant, P.; Nectoux, P.; Dalbiez, J. P. *Rev. Phys. Appl.* **1981**, *16*, 19−33.
(29) Rhee, K. W.; Ware, B. R. *J. Chem. Phys.* **1983**, *78*, 3349−3353.
(30) Grossman, P. D.; Soane, D. S. *Anal. Chem.* **1990**, *62*, 1592−1596.
(31) Bernard, O.; Turq, P.; Blum, L. *J. Phys. Chem.* **1991**, *95*, 9508−9513.
(32) Strege, M.; Lagu, A. *Anal. Chem.* **1991**, *63*, 1233−1236.
(33) Hoss, U.; Batzill, S.; Deggelmann, M.; Graf, C.; Hagenbuchle, M.; Johner, C.; Kramer, H.; Martin, C.; Overbeck, E.; Weber, R. *Macromolecules* **1994**, *27*, 3429−3431.
(34) Rasmusson, M.; Åkerman, B. *Langmuir* **1998**, *14*, 3512−3516.
(35) Alfrey, T., Jr.; Morawetz, H.; Fitzgerald, E. B.; Fuoss, R. M. *J. Am. Chem. Soc.* **1950**, *72*, 1864.
(36) Strauss, U. P.; Gershfeld, N. L.; Spiera, H. *J. Am. Chem. Soc.* **1954**, *76*, 5909−5911.
(37) Nagasawa, M.; Soda, A.; Kagawa, I. *J. Polym. Sci.* **1958**, *31*, 439−451.
(38) Noda, I.; Nagasawa, M.; Ota, M. *J. Am. Chem. Soc.* **1964**, *86*, 5075−5079.

(39) Takahashi, T.; Noda, I.; Nagasawa, M. *J. Phys. Chem.* **1970**, *74*, 1280−1284.
(40) Nagasawa, M.; Noda, I.; Takahashi, T.; Shimamoto, N. *J. Phys. Chem.* **1972**, *76*, 2286−2294.
(41) van der Drift, W. P. J. T.; Overbeek, J. T. G. *J. Colloid Interface Sci.* **1979**, *71*, 79−92.
(42) Wilcoxon, J. P.; Schurr, J. M. *J. Chem. Phys.* **1983**, *78*, 3354−3364.
(43) Zero, K.; Ware, B. R. *J. Chem. Phys.* **1984**, *80*, 1610−1615.
(44) Whitlock, L. R. In *New Directions in Electrophoretic Methods;* ACS Symposium Series 335; Jorgenson, J. W., Phillips, M., Eds.; American Chemical Society: Washington, DC, 1987; pp 222−245.
(45) Dalbiez, J. P.; Tabti, K.; Derian, P. J.; Drifford, M. *Rev. Phys. Appl.* **1987**, *22*, 1013−1024.
(46) Turco, G. P. Ph.D. Thesis, University of Wisconsin, 1992.
(47) Xia, J.; Dubin, P. L.; Havel, H. A. *Macromolecules* **1993**, *26*, 6335−6337.
(48) Wiersema, P. H.; Loeb, A. L.; Overbeek, J. T. G. *J. Colloid Interface Sci.* **1966**, *22*, 78−99.
(49) Overbeek, J. T. G.; Wiersema, P. H. In *Electrophoresis; Theory, Methods, and Applications;* Bier, M., Ed.; Academic Press: New York, 1967; Vol. II.
(50) Dukhin, S. S.; Derjaguin, B. V. *Electrokinetic Phenomena*; John Wiley & Sons: New York, 1974; Vol. 7.
(51) Sherwood, J. D. *J. Chem. Soc., Faraday Trans. 2* **1982**, *78*, 1091−1100.
(52) Manning, G. S. *J. Phys. Chem.* **1980**, *84*, 1059.
(53) Manning, G. S. *Q. Rev. Biophys.* **1978**, *11*, 179−246.
(54) Manning, G. S. *J. Phys. Chem.* **1981**, *85*, 1506−1515.
(55) Schellman, J. A.; Stigter, D. *Biopolymers* **1977**, *16*, 1415−1434.
(56) Stigter, D. *J. Phys. Chem.* **1978**, *82*, 1417−1423.
(57) Stigter, D. *J. Phys. Chem.* **1978**, *82*, 1424−1429.
(58) Stigter, D. *J. Phys. Chem.* **1979**, *83*, 1663−1670.
(59) Stigter, D. *J. Phys. Chem.* **1979**, *83*, 1670−1675.
(60) Völkel, A. R.; Noolandi, J. *J. Chem. Phys.* **1995**, *102*, 5506−5511.
(61) Allison, S. A.; Mazur, S. *Biopolymers* **1998**, *46*, 359−373.
(62) Hermans, J. J. *J. Polym. Sci.* **1955**, *18*, 527−534.
(63) Hermans, J. J.; Fujita, H. *Proc. Akad. Amsterdam* **1955**, *B58*, 182−187.
(64) Overbeek, J. T. G.; Stigter, D. *Recl. Trav. Chim. Pays-Bas* **1956**, *75*, 543−554.
(65) Mills, R. A. *Biopolymers* **1970**, *9*, 1511−1530.
(66) Imai, N.; Iwasa, K. *Isr. J. Chem.* **1973**, *11*, 223−233.
(67) Schmitt, A.; Meullenet, J. P.; Varoqui, R. *Biopolymers* **1978**, *17*, 413−423.
(68) Schmitt, A.; Meullenet, J. P.; Varoqui, R. *Biopolymers* **1978**, *17*, 1249−1255.
(69) van der Drift, W. P. J. T.; de Keizer, A.; Overbeek, J. T. G. *J. Colloid Interface Sci.* **1979**, *71*, 67−78.
(70) Long, D.; Viovy, J.-L.; Ajdari, A. *J. Phys.: Condens. Matter* **1996**, *8*, 9471−9475.
(71) Long, D.; Viovy, J.-L.; Ajdari, A. *Phys. Rev. Lett.* **1996**, *76*, 3858−3861.
(72) Allison, S. A.; Nambi, P. *Macromolecules* **1992**, *25*, 3971−3978.
(73) Allison, S. A.; Nambi, P. *Macromolecules* **1994**, *27*, 1413−1422.
(74) Cosgrove, T.; Obey, T. M.; Ryan, K. *Colloids Surf.* **1992**, *65*, 1−7.
(75) Nierlich, M.; Boué, F.; Lapp, A.; Oberthur, R. *J. Phys. (Paris)* **1985**, *46*, 649−655.
(76) Davis, R. M.; Russel, W. B. *Macromolecules* **1987**, *20*, 518−525.
(77) Record, M. T.; Woodbury, C. P.; Lohman, T. M. *Biopolymers* **1976**, *15*, 893−915.
(78) Tinland, B.; Pluen, A.; Sturm, J.; Weill, G. *Macromolecules* **1997**, *30*, 5763−5765.
(79) Mondescu, R.; Muthukumar, M. To be submitted for publication.

MA9903761